



Thin film pyrolytic carbon electrodes: A new class of carbon electrode for electroanalytical sensing applications

Gareth P. Keeley^{a,b}, Niall McEvoy^{a,c}, Shishir Kumar^{a,b}, Nikos Peltekis^{a,b},
Marcel Mausser^{a,b}, Georg S. Duesberg^{a,b,*}

^a Centre for Research on Adaptive Nanostructures and Nanodevices (CRANN), Dublin 2, Ireland

^b School of Chemistry, Trinity College, Dublin 2, Ireland

^c School of Physics, Trinity College, Dublin 2, Ireland

ARTICLE INFO

Article history:

Received 19 April 2010

Received in revised form 12 May 2010

Accepted 17 May 2010

Available online 24 May 2010

Keywords:

Pyrolytic carbon

Voltammetry

Impedance spectroscopy

Electro-catalysis

Materials science

ABSTRACT

This communication describes the electrochemical properties of thin pyrolytic carbon (PyC) films created using a reliable, non-catalytic chemical vapour deposition (CVD) process. After deposition, the electron transfer characteristics of the films are optimised using a simple oxygen plasma treatment. The redox probes $\text{Ru}(\text{NH}_3)_6^{3+/2+}$, $\text{Fe}(\text{CN})_6^{3-/4-}$ and $\text{Fe}^{3+/2+}$ are employed to demonstrate that the resulting material is endowed with a large electrochemical surface area and outstanding electron transfer properties. Atomic force microscopy (AFM), Raman and X-ray photoelectron spectroscopy (XPS) are used to elucidate the morphology and chemical composition of the electrode surfaces. This material represents a new class of carbon electrode, and its large densities of edge-plane sites and oxygenated functionalities make it an ideal candidate for electrochemical sensor applications.

© 2010 Elsevier B.V. All rights reserved.

1. Introduction

Carbon materials are widely used in electrochemistry due to their low cost, wide potential window and electro-catalytic activity [1]. Their applications in electro-catalysis depend very much on their microstructure and surface chemistry, and the various allotropes have very different electrochemical properties. The electrochemistry of 'traditional' sp^2 -hybridised carbon materials such as glassy carbon and highly-ordered pyrolytic graphite has been thoroughly probed. The last decade has seen an extraordinary amount of research into the electrochemical properties of carbon nanotubes [2–4], and recent years have seen the emergence of graphene-based electrodes [5–13].

Pyrolytic carbon is a form of nano-crystalline graphite made by the non-catalytic CVD of hydrocarbon precursors. These conductive, thermally stable thin films are composed of small graphitic crystallites (1–2 nm). This material has been known for decades [14] and its growth mechanism has been described by Dong and Hüttinger [15]. In the past it has been used in lithium batteries [16] and integrated as an electrode material in dynamic random access memory cell capacitors [17]. Despite this, very little is known of the fundamental electron transfer characteristics of PyC films. Hadi et al. have reported electrodes based on PyC grown on graphite rods, which were optimised using anodic activation [18] and laser irradiation [19]. In

this communication, the electrochemical properties of thin PyC films grown on insulating substrates are presented for the first time. The films are fabricated by the CVD of ethyne on SiO_2 wafers and their electrochemical activity is optimised using a simple oxygen plasma treatment. The resulting material is shown to be endowed with low background current, large electrochemical surface area and outstanding electron transfer properties.

2. Experimental

2.1. Reagents and equipment

All chemicals were purchased from *Sigma-Aldrich*. All solutions were prepared using water (resistivity 18.2 $\text{M}\Omega\text{ cm}$). AFM was performed using a *Nanoscope III Multimode* instrument (Digital Instruments, Santa Barbara, CA). A *Gamry 600* potentiostat was used to perform electrochemical measurements, along with a three-electrode configuration. *IJ Cambria* supplied platinum wire counter electrodes and Ag/AgCl reference electrodes. Pyrolytic carbon films were used as working electrodes. These were incorporated into the electrochemical cell by placing the substrates in an electrode designed in-house, resulting in PyC disc working electrodes of radius 1.5 mm. Electrolytes were purged for 20 min using high-purity Ar before experiments, and a blanket of Ar was maintained over the solution during measurements. All electrochemical experiments were performed at room temperature.

* Corresponding author. Centre for Research on Adaptive Nanostructures and Nanodevices (CRANN), Dublin 2, Ireland. Tel.: +353 1 896 3035; fax: +353 1 896 3037.
E-mail address: duesberg@tcd.ie (G.S. Duesberg).

2.2. Formation and plasma treatment of PyC films

PyC films were grown on SiO₂ (300 nm) substrates in a furnace at 950 °C, using ethyne as the precursor. The deposition tube was 10 cm in diameter and 125 cm in length (heated region of 75 cm). The pressure and residence time were 20 Torr and 30 min, respectively. Substrates were then cooled under nitrogen flow. Film thicknesses were found to be approximately 400 nm under these conditions. Oxygen plasma etching was carried out using a R³T TWR-2000 T microwave radical generator with an output power of 1 kW at 0.8 Torr. A 10 min etch was found to reduce the film thickness to 150 nm. Shorter times resulted in some improvement in electron transfer properties, but a 10 min period was found to be optimum. Longer dwell times had no further effect on electrochemical characteristics, and four-point probe measurements indicated that exposure periods of 20 min or more resulted in the removal of the carbon material. All films hereafter referred to as 'etched' were treated for 10 min.

3. Results and discussion

3.1. Electrochemical surface area of PyC electrodes

The etching process was found to increase the electrochemically active surface area of the PyC films. The Ru(NH₃)₆^{3+/2+} probe was used to quantify this increase, and Fig. 1 shows a typical comparison between as-grown and etched electrodes. The larger peak current for the latter is attributed to a greater electrochemically active area. Etching was found to increase this area from 0.11 to 0.14 cm², based on a Ru(NH₃)₆^{3+/2+} diffusion coefficient of 6.2 × 10⁻⁶ cm² s⁻¹ [20] and peak current values obtained at 100 mV s⁻¹. It is noted that, due to roughness, both of these values are larger than the geometric area of the electrodes (0.07 cm²). The voltammetric data is supported by the AFM images of 2 × 2 μm areas included in Fig. 1, which clearly show the greater roughness of the etched surface. The root-mean-square roughness over the measured areas was found to increase from 0.99 to 3.32 nm.

3.2. Electron transfer properties of PyC electrodes

The Fe(CN)₆^{3-/4-} probe was used to elucidate the electron transfer characteristics of the PyC films. Fig. 2(a) compares voltammograms obtained using as-grown and etched electrodes. It is clear that the electron transfer at the as-grown film is sluggish, with a large peak separation (~350 mV) at a sweep rate of 100 mV s⁻¹. In contrast, the

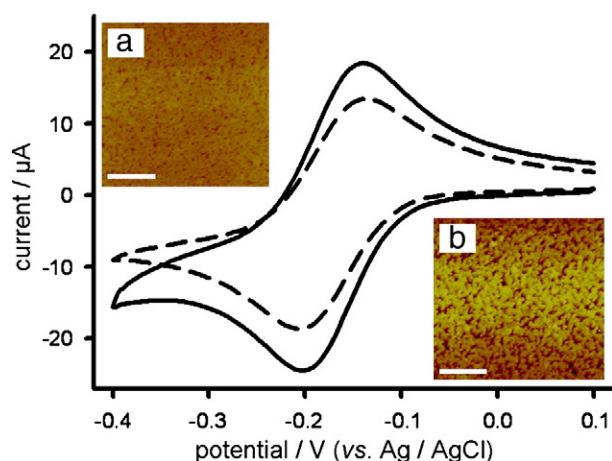


Fig. 1. Voltammograms recorded at as-grown (dashed) and etched (solid) PyC in 1 mM Ru(NH₃)₆³⁺ in 1 M KCl at 100 mV s⁻¹. Insets (a) and (b) show typical AFM images of the as-grown and etched surfaces, respectively.

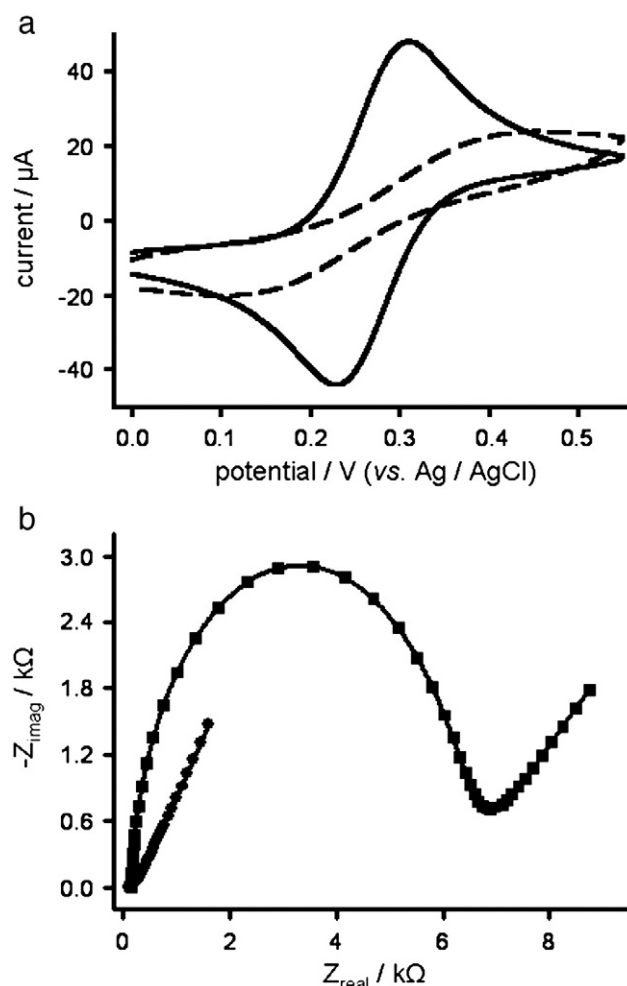


Fig. 2. (a) Voltammograms recorded at as-grown (dashed) and etched (solid) PyC in 1 mM Fe(CN)₆^{3-/4-} in 1 M KCl at 100 mV s⁻¹. (b) Nyquist plots recorded at as-grown (■) and etched (●) PyC at +0.26 V when an AC signal (10 mV) was applied in the range of 10⁻¹ to 10⁵ Hz.

etched electrode gives rise to well-defined peaks with a small ΔE_p value of 80 mV, suggesting a dramatic enhancement in the electron transfer rate. Voltammetric peak currents were found to increase linearly with the square root of scan rate (data not shown), indicating a diffusion-controlled process. In order to provide a quantitative insight into the electron transfer properties of the etched PyC, the standard electrochemical rate constant was calculated for the Fe(CN)₆^{3-/4-} test reaction. This was done using the Nicholson [21] method, which yielded a value of 0.013 cm s⁻¹. A detailed description of the application of this method can be found in previous work [22]. It is worth noting that this value is an order of magnitude higher than those reported by Pacios et al. [23] for a range of carbon nanotube composite electrodes, using the same approach.

The enhanced electron transfer properties of the etched PyC surfaces were also clear from impedance spectroscopy data. Fig. 2(b) shows a comparison between Nyquist plots obtained using as-grown and etched electrodes. In such plots, the resistance to charge transfer is indicated by the size of the semicircular region. It can be seen that the response of the as-grown film is dominated by this feature, suggesting that the reaction kinetics are controlled by electron transfer at all frequencies. However, the etched electrode gives rise to a far smaller resistance, with a considerable linear region indicating diffusion control at moderate frequencies. The impressive properties of the etched electrodes are attributed to their high density of edge-plane sites and defects, which have been established as key

participants in the promotion of electron transfer at carbon electrodes [24–27]. It is suggested that, as well as increasing the electrochemical surface area, the effect of etching is to rupture the nano-crystalline structure of PyC. This could create a smaller crystal size and expose a greater proportion of edges, leading to enhanced rates of electron transfer. The kinetics of the $\text{Fe}(\text{CN})_6^{3-/4-}$ reaction are known to be very sensitive to the amount of edge-plane graphite on electrode surfaces [26].

3.3. Oxygenated functionalities on etched PyC electrodes

As well as creating a higher density of edge-plane sites and defects on the PyC films, the etching procedure employed in this study was found to increase the oxygen content of the electrode surface. This was shown using XPS. Fig. 3 shows that there is an increase in the oxygen signal after etching. Also, the high-resolution spectrum of C_{1s} changes (data not shown). The as-grown PyC films exhibit an asymmetric peak centred at 284.7 eV, with a long tail extended to the higher-energy region. Such a peak is a characteristic of aromatic structures with delocalised π electrons [28,29]. The etched films also give rise to this signal, but here the tail shows evidence of oxygen-related functionalities. Analytical de-convolution revealed the presence of hydroxyl, carbonyl and carboxylic acid functionalities, in accordance with previous reports [30–32]. The functionalisation of the PyC films was confirmed electrochemically, using the $\text{Fe}^{3+/2+}$ probe. The kinetics of this redox process are known to be strongly influenced by the presence of surface oxides [1]. The upper inset of Fig. 3 shows voltammograms recorded at PyC electrodes before and after etching. The as-grown films show no response to this probe, whereas etched films give rise to ideal voltammograms, indicative of rapid electron transfer. This effect is attributed to the large oxide coverage generated by etching. Also contained in Fig. 3 is a Raman spectrum recorded for an as-grown film. As with other graphitic materials, the primary features are the *D* and *G* peaks at 1350 and 1580 cm^{-1} , respectively. The former is related to defects and disorder, and its prominence is indicative of the nano-crystalline nature of these electrodes. Etching had no effect on the Raman

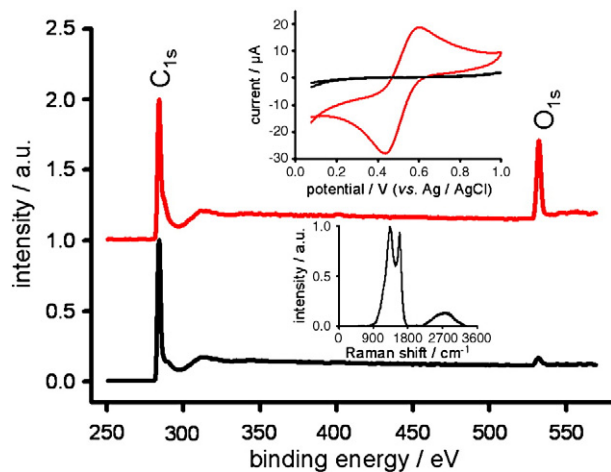


Fig. 3. XPS surveys of as-grown (black) and etched (red) PyC. Upper inset shows voltammograms recorded at these electrodes in 5 mM $\text{Fe}^{3+/2+}$ in 0.2 M HClO_4 at 100 mV s^{-1} . Lower inset shows a Raman spectrum recorded for as-grown PyC.

spectrum, despite the considerable change found using XPS. We attribute this to the large penetration (100 nm) of the Raman laser. For such thin films, Raman can be thought of as a bulk technique, whereas XPS only penetrates to 1 nm.

4. Conclusions

For the first time, the fundamental electron transfer characteristics of thin PyC films grown on insulating substrates have been explored. The electrochemical activity of these surfaces is optimised using a simple plasma etching process, yielding electrodes endowed with large electrochemical surface areas, low background current and outstanding electron transfer properties. Their increased density of edge-plane sites and defects, in combination with their extensive functionalisation, makes them ideal electrodes for electroanalytical sensors with low detection limits, and as immobilisation platforms for redox proteins in amperometric biosensors. The films can be made cheaply and on a large scale, permitting the production of disposable, high-performance electrochemical electrodes.

Acknowledgements

This work was supported by Science Foundation Ireland under the CSET scheme and the Embark initiative under the IRCSET scheme.

References

- [1] R.L. McCreery, Chem. Rev. 108 (2008) 2646–2687.
- [2] J. Wang, Electroanalysis 17 (2005) 7–14.
- [3] J.J. Gooding, Electrochim. Acta 50 (2005) 3049–3060.
- [4] I. Dumitrescu, P.R. Unwin, J.V. Macpherson, Chem. Commun. (2009) 6886–6901.
- [5] L. Tang, Y. Wang, Y. Li, H. Feng, J. Lu, J. Li, Adv. Funct. Mat. 19 (2009) 2782–2789.
- [6] N.G. Shang, P. Papakonstantinou, M. McMullan, M. Chu, A. Stamboulis, A. Potenza, S.S. Dhesi, H. Marchetto, Adv. Funct. Mater. 18 (2008) 3506–3514.
- [7] T.T. Baby, S.S. Jyothirmayee Aravind, T. Arockiadoss, R.B. Rakhii, S. Ramaprabhu, Sens. Actuators B: Chem. 145 (2010) 71–77.
- [8] H. Liu, J. Gao, M. Xue, N. Zhu, M. Zhang, T. Cao, Langmuir 25 (2009) 12006–12010.
- [9] J.-F. Wu, M.-Q. Xu, G.-C. Zhao, Electrochem. Commun. 12 (2009) 175–177.
- [10] Y. Wang, Y. Wan, D. Zhang, Electrochem. Commun. 12 (2010) 187–190.
- [11] C. Shan, H. Yang, J. Song, D. Han, A. Ivaska, L. Niu, Anal. Chem. 81 (2009) 2378–2382.
- [12] Y. Wang, Y. Li, L. Tang, J. Lu, J. Li, Electrochem. Commun. 11 (2009) 889–892.
- [13] M. Zhou, Y. Zhai, S. Dong, Anal. Chem. 81 (2009) 5603–5613.
- [14] A. Oberlin, Carbon 40 (2002) 7–24.
- [15] G.L. Dong, K.J. Hüttinger, Carbon 40 (2002) 2515–2528.
- [16] M. Mohri, N. Yanagisawa, Y. Tajima, H. Tanaka, T. Mitate, S. Nakajima, M. Yoshida, Y. Yoshimoto, T. Suzuki, H. Wada, J. Power Sources 26 (1989) 545–551.
- [17] G. Aichmayr, A. Avellán, G.S. Duesberg, F. Kreupl, S. Kudelka, M. Liebau, A. Orth, A. Sänger, J. Schumann, O. Storbeck, VLSI (2007).
- [18] M. Hadi, A. Rouhollahi, M. Yousefi, F. Taidy, R. Malekfar, Electroanalysis 18 (2006) 787–792.
- [19] M. Hadi, A. Rouhollahi, F. Taidy, M. Yousefi, Electroanalysis 19 (2007) 668–673.
- [20] A.F. Holloway, K. Toghiani, G.G. Wildgoose, R.G. Compton, M.A.H. Ward, G. Tobias, S. A. Llewellyn, B.N. Ballesteros, M.L.H. Green, A. Crossley, J. Phys. Chem. C 112 (2008) 10389–10397.
- [21] R.S. Nicholson, Anal. Chem. 37 (1965) 1351–1355.
- [22] M.E.G. Lyons, G.P. Keeley, Sensors 6 (2006) 1791–1826.
- [23] M. Pacios, M. del Valle, J. Bartroli, M.J. Esplandiú, J. Electroanal. Chem. 619 (2008) 117–124.
- [24] A.C. Ferrari, J.C. Meyer, V. Scardaci, C. Casiraghi, M. Lazzeri, F. Mauri, S. Piscanec, D. Jiang, K.S. Novoselov, S. Roth, A.K. Geim, Phys. Rev. Lett. 97 (2006) 187401.
- [25] A. Chou, T. Böcking, N.K. Singh, J.J. Gooding, Chem. Commun. (2005) 842–844.
- [26] R.J. Rice, R.L. McCreery, Anal. Chem. 61 (1989) 1637–1641.
- [27] R.R. Moore, C.E. Banks, R.G. Compton, Analyst 129 (2004) 755–758.
- [28] P.M.Th.M. van Attekum, G.K. Wertheim, Phys. Rev. Lett. 43 (1979) 1896–1898.
- [29] A. Dekanski, J. Stevanović, R. Stevanović, Branislav Ž. Nikolić, Vladislava M. Jovanović, Carbon 39 (2001) 1195–1205.
- [30] E. Desimoni, G.I. Casella, A. Morone, A.M. Salvi, Surface and Interface Analysis 53 (1982) 627–634.
- [31] Y. Xie, P.M.A. Sherwood, Appl. Spectrosc. 43 (1989) 1153–1158.
- [32] Y. Xie, P.M.A. Sherwood, Chem. Mater. 2 (1990) 293–299.